Double Scaffold Networks Regulate Edible Pickering Emulsion Gel for Designing Thermally Actuated 4D Printing

Qinbo Jiang,[1] Bernard P. Binks[2] and Zong Meng[1,*]

[1] *State Key Laboratory of Food Science and Technology, School of Food Science and Technology, Jiangnan University, 1800 Lihu Road, Wuxi 214122, Jiangsu, China*

[2] *Department of Chemistry, University of Hull, Hull. HU6 7RX. UK*

* Corresponding author: mengzong@jiangnan.edu.cn

Contains ESI

Submitted to: ? on ?.2.22

Keywords: double networks, edible 3D printing, 4D printing, water-in-oil Pickering emulsion gel, rigid porous biomaterial

Abstract

3D and 4D printing of emulsion gels can be achieved by controlling the continuous phase and the interface. Edible high internal phase water-in-oil Pickering emulsion gels (PEGs) with a tunable double scaffold network structure are designed and prepared by food-grade phytosterol nanoparticles (PPs). In PEGs, PPs through hydrogen bonding enable binding of emulsion droplets to form the first scaffold network, giving PEGs high viscoelasticity for 3D printing. In the continuous oil phase, palm kernel stearin (PKST) can crystallize forming the second scaffold network of crystals to reinforce 3D printed objects of PEGs. The PEG can be used as a biocompatible template to engineer edible and rigid porous materials with adjustable strength and pore size depending on the degree of curing. 4D printing of PEGs is achieved by the thermal response of the PKST crystal network, leading to the unlimited potential of highly biocompatible PEGs in many applications.

1. Introduction

Incorporation of two different liquids and the presence of gel characteristics of emulsion gels endow the jammed dispersion with unique viscoelasticity and thixotropy, promoting emulsion gels to be attractive materials in colloid science areas such as food, medicine, cosmetics and chemical engineering.[1, 2] The interfacial functionality and the uniform dispersion of emulsion droplets advance the applicability of emulsion gels in extended interfacial catalysis, bioactive component delivery, environmentally friendly paint, *etc*.[3-6] The gelation of emulsions enhances emulsion stability by delaying or preventing creaming, Ostwald ripening and coalescence.[7] Moreover, gelation endows emulsions with high viscoelasticity highly related to plasticity.

3D printing has been developed for some years and enables one to overcome many challenges facing the traditional manufacturing industry.[8, 9] With the development of material science, the application scene of 3D printing has been continuously enlarged by novel inks and the role of 3D printing technology is constantly redefined by emerging areas, such as intelligence manufacturing and biological engineering based on the real-time modeling and rapid prototyping technology.[10, 11] However, in the field of edible materials, the adaptation of advanced technologies and 3D printing has certain limitations. For example, selective laser

sintering could offer a high temperature to melt materials for high precision printing which may not be appropriate for many edible materials.[12] Direct ink writing (DIW) has the limitation for rheological properties of the ink that the thixotropy and structural recovery ability are needed to ensure the printability of ink materials and the formability of ejected filaments.[13] Edible materials that support DIW 3D printing without adjusting the temperature contain some mashed vegetables and gelatinous substances, but the strength of printed objects is low which limits the application.[14, 15] Edible oil-in-water Pickering emulsion gels have the distinctive viscoelasticity for 3D printing, but they require high internal phase volume fractions which increases the content of total lipid intake raising the risk of obesity and cardiovascular diseases.[16-20] In addition, the critical role of the continuous phase in oil-in-water emulsions in controlling the physical properties of the edible ink is difficult to judge. It is of great importance to design an edible Pickering emulsion gel which can significantly lower the oil volume fraction, fit DIW and engineer the continuous phase as the scaffold to support printed objects.

Hence, a novel high internal phase water-in-oil Pickering emulsion gel (PEG) containing 75% water was designed stabilized by phytosterol nanoparticles (PPs). The oil phase can be a mixture of soybean oil and palm kernel stearin (PKST) allowing us to regulate the physical properties of PEGs due to the crystallization ability of PKST. The effect of the content of PKST in the oil phase on the properties of the PEG was investigated. Since PPs are hydrophobic, they adsorb to the oil-water interface to stabilize a water-in-oil Pickering emulsion, jamming emulsion droplets from free migration and enabling droplets to become the building block of the emulsion gel network for DIW 3D printing. The scaffold of PEGs was created by the fat crystal network of PKST in the continuous phase, which was combined with real-time scanning modeling equipment (3D scanning imager) to explore the rapid customization of 3D printing in DIW. In addition, an edible rigid porous material with adjustable properties was constructed using PEGs as the template. Based on the thermal sensitivity of the PKST crystal network and the rheological properties of PEGs, intelligent controlling 4D printing of PEGs was carried out by the thermal-actuated design, and the partial replacement of PEG for cocoa butter in 4D printed chocolate was applied for merging the advanced technology with chocolate processing.

2. Results and Discussion

2.1. PEGs

A Pickering emulsion is stabilized by the irreversible adsorption of colloidal particles at the oil-water interface. Water-in-oil emulsions require particles to be reasonably hydrophobic. Phytosterols belong to triterpenes, containing a tetracyclic ring (three six-membered rings and one five-membered ring) and are extracted from natural plants. The main components include β-sitosterol, rapeseed oil sterol, rapeseed sterol, stigmasterol, *etc*.[21] Because of the presence of two kinds of hydrophobic groups (cyclic hydrocarbon, long hydrocarbon chain) and hydrophilic groups (hydroxyl), phytosterols are potentially surface-active. The unique crystallization ability can make dissolved phytosterols recrystallize to form nanoparticles.[22] PPs prepared by an anti-solvent precipitation method were flake-like with an equivalent diameter of about 1100 nm and a thickness of about 105 nm (Figure S1). The contact angle of a water drop under soybean oil on a substrate of PPs was 150° (Figure S2). now need to describe a typical emulsion composition: what's in water, what's in oil, PPs concentration, how made *etc*. making reference to Figure 1ai The addition of κ-carrageenan (κ-CA) in the aqueous phase improved its stability in PEGs by gelling it.[23, 24] According to confocal and optical micrographs (Figure S3 which part of this figure do you refer to?), water emulsion droplets in the PPs-stabilised PEG were densely packed and limited the relative movement of the whole system resulting in its high viscoelasticity (Figure 1aii, iii). you must describe 1aiv separately In Figure 1av, the SEM image of a dried PEG, where the oil phase and water phase have been removed, shows that interfacial PPs form a cellular skeleton to protect droplets from coalescence. Due to the high density of emulsion droplets, PPs can interact do you mean with each other? between droplets? through hydrogen bonding to reinforce the particulate-based gel network. The gel network is part of the double scaffold system. Because PPs are crystalline, PPs on the interface of droplets could be observed using polarized light microscopy (Figure S3c(iv)) no-you need to cite each part of a figure in order in the paper.The Fourier transform infrared (FTIR) spectra (Figure 1b and 1c) show the infrared absorption of PPs, κ-CA powder and dried PEG, respectively. The stretching vibration of the -OH group in PPs appeared at 3429 and 3334 cm^{-1}, while it appeared at 3423 cm^{-1} for κ-CA. However, only two separated peaks appeared at 3414 and 3321 cm^{-1} for the dried PEG meaning the occurrence of a redshift. This is attributed to the hydrogen bonding between PPs and κ-CA molecules. The adsorption of flake-like PPs at the interface is slightly

different to that of spherical particles and the desorption energy reads:[25]

$$\Delta G = S\gamma_{wo}\left(1+\cos\theta\right) \quad (1)$$

where S is the interfacial area covered by PPs, γ_{wo} best to have γ_{ow} is the bare oil-water interfacial tension (for soybean oil it is 23.7 ± 0.1 mN/m this is very low, normally around 30..; have you measured it?) and θ is the three-phase contact angle which particles adopt at the interface. are plate-like particles adsorbed with their faces parallel to the interface? The desorption PPs was assumed to be towards the oil phase. The calculated desorption energy of PPs was about 1.8×10^8 kT, which is much higher than the thermal energy meaning the attachment of PPs at the interface was extremely strong.[26]

you must mention the long-term stability of the PEGs: no sedimentation of oil or coalescence of water?

you do not seem to say any more about κ-CA: do you need to gel the droplets for printing? have you tried without polymer?

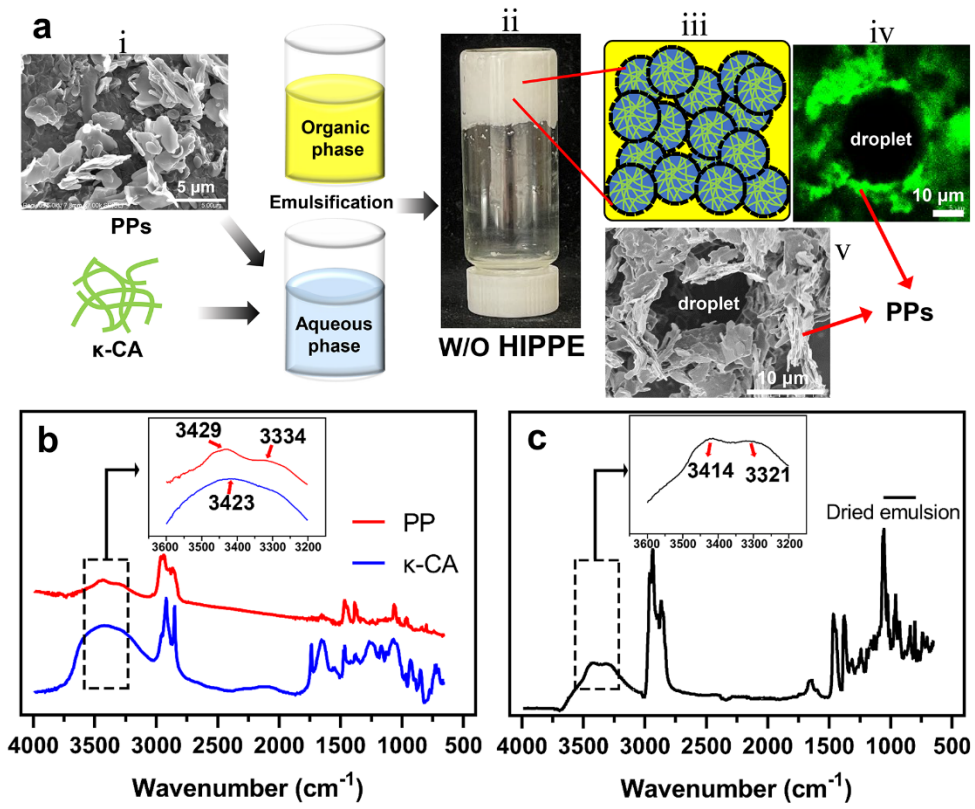

Figure 1. (a) Illustration of PEG preparation and microstructure. (i) SEM image of PPs, (ii) appearance of a PEG, (iii) sketch of PEG microstructure, (iv) CLSM image of emulsion droplet,

(v) SEM image of dried PEG. PPs are dyed by Rhodamine B as green in CLSM. (b, c) FTIR spectra of PPs, κ-CA and dried PEG (only having PPs and κ-CA what does this bracket mean?) respectively, and insets are from the region 3600 to 3200 cm^{-1}.

are all the PEGs in Figure 1 without PKST. this must be made clear

2.2. DIW 3D printability

The 3D printing method of DIW requires that the ink has good printability (extrusion fluidity) and formability (plasticity). The scaffold network formed by the dense accumulation of droplets and the hydrogen bonding among PPs makes the system viscoelastic to meet the 3D printing requirements. However, for 3D printing, the temperature of the ink storage tank must be controlled to limit or prevent? the formation of PKST crystals. Hence, the DIW printing test maintained the ink temperature at 45 °C to prevent PKST in the oil phase from solidifying and enabling the printability of PEGs (Figure 2a). The temperature of the rheological testing of PEGs was also set to 45 °C. As a high internal phase emulsion, the small amplitude oscillation test (Figure 2b) showed that the elastic modulus (G') of all PEGs in the linear viscoelastic region was much larger than the viscous modulus (G"), implying that the PEG was a viscoelastic solid. An increase in the proportion of PKST in soybean oil leads to higher values of both G' and G" of PEGs, meaning that PKST is conducive to enhancing the solid-like properties. At higher strain, the inversion of G' and G" occurred first in the PEG without PKST such that G" was significantly higher than G' when the strain was 100%. The strain that resulted in the inversion of G' and G" increased as the content of PKST increased, while the gap between G' and G" decreased at 100%. This pseudoplastic feature showed that the PEG was a thixotropic fluid and had excellent fluidity when subjected to high strain, which matched the 3D printability of PEGs. However, the average droplet size of PEGs was around 10 μm at different PKST proportions in the oil phase (Figure S3a). In DIW printing, the rheological state of PEGs in the ink storage tank was similar to that in the linear viscoelastic region, in which PEGs suffered a minor strain. In this state, PEGs in the ink storage tank behave like a viscoelastic solid. The rheological state of PEGs extruded at the nozzle of the printer is similar to that suffered at high strain, in which G' of PEGs is lower than G" to obtain the ideal fluidity and improve the fluency and printability of the ink.[27]

The plasticity of inks after being ejected is one of the essential factors in DIW printing.[28]

Although many food-grade systems display shear-thinning ability, their structural recovery ability is quite different after shear damage. If the structural recovery ability (plasticity) is weak, the material cannot be quickly formed in 3D printing which would result in printing failure. A three-stage strain jump sweep of PEGs was carried out to simulate the three states of PEGs in the 3D printing process: (i) A state of slowly creeping down of PEGs in the ink storage tank when subjected to slight shear; (ii) a state of PEGs suffering from strong shear at the nozzle during rapid ink ejection; (iii) a state in which PEGs remain still and stacked on the plate. As shown in Figure 2c, G' of PEGs was significantly higher than G" when the strain was 0.01% in stage (i) simulating the state in the ink storage tank, indicating that PEGs were viscoelastic before being ejected. In stage (ii), G" of PEGs exceeded G' as the strain suddenly increased to 100%, simulating the state of ejecting PEGs, showing that PEGs had excellent fluidity when printed. In stage (iii), G' of PEGs was restored and surpassed G" again when the strain was back to 0.01%, simulating piling up of PEGs statically in the printed object, showing that PEGs had a fast structural recovery speed and good plasticity. The general rheological behavior of all PEGs was the same, and the substitution of soybean oil by PKST did not affect the plasticity of PEGs after being ejected (Figure 2d).

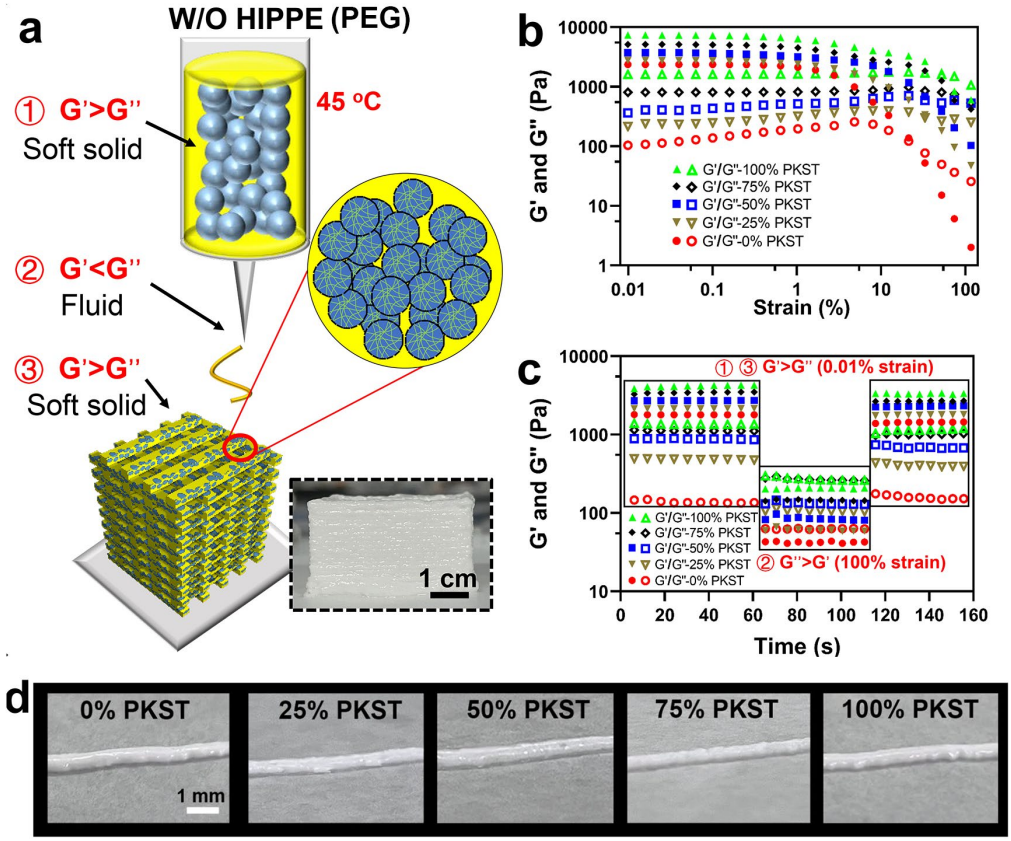

Figure 2. (a) Sketch of the 3D printing process using PEGs with the ink storage tank at 45 ºC, inset photo' needs mentioning (b) rheological strain sweep of PEGs containing different proportions of PKST in soybean oil at 45 °C, (c) a three-stage strain jump sweep at 45 °C of above PEGs for simulating the 3D printing process. First and third stages had 0.01% strain while second stage had 100% strain, (d) appearance of PEG printed strips ejected by the 0.85 mm nozzle of the 3D printer for the above emulsions.

2.3. Scaffold reinforcing in continuous oil phase

you need to refer to Figure S4 here and say that soybean oil remains liquid but that PKST can crystallise. what is the melting range for PKST? I can't tell from Figure S4 what happens at 45 °C – the temp. for rheology measurements! The application of emulsions is extensive, and it is often beneficial to enhance the physical properties of emulsions under different scenarios. For most oil-in-water emulsions, hydrocolloids with excellent thickening effects were commonly used as additives to gel the external phase.[29] However, in water-in-oil emulsions, the enhancement of the continuous phase requires lipophilic materials as effective structural agents, such as ethylcellulose.[30] Natural vegetable fats are the ideal structure enhancer for liquid oils because many triglycerides with high saturation and high melting point can

crystallize and self-assemble into a crystal network at a controlled temperature.[31] PKST used in this work is the natural vegetable fat from palm plants, a component with a high melting point extracted from palm oil. PKST has a high hardness and has been widely used in foods such as shortening and margarine.[32] For PEGs, besides the scaffold network formed by the stack of emulsion droplets and the interaction of PPs, the continuous phase could also be constructed to be a rigid framework as a second scaffold. Through the unique crystal network formed by the hydrogen bonding-induced I thought crystals in oil interact mainly through van der Waals interactions? self assembly among triglyceride crystals in PKST, the continuous phase can be transformed from liquid to solid. Hence, PKST can partially replace soybean oil as the continuous phase of PEGs to reinforce the oil phase by controlling the temperature (Figure 3a). The transformation of the continuous phase from liquid to solid depends on the crystal network formed by the high melting point triglycerides in PKST after crystallization. Fat crystals were formed in the oil phase and interacted with each other driven by hydrogen bonds,[33] and the dense stack of fat crystals hinder their movement by building crystal clusters. With the complete solidification of the continuous phase, the internal water droplets would be further fixed. This fat crystal scaffold network becomes the basis for the preparation of food-grade rigid porous materials.

The reinforcing effect of PKST in PEGs can be traced by the rheological cooling sweep (Figure 3b). In the sweep, the temperature gradually decreased from 50 ºC to 20 ºC. At 50 ºC, G' and G" of all PEGs were less than 10,000 and 1,000 Pa, respectively. Then triglycerides in PKST began to crystallize and solidify the oil phase when the temperature fell. The formation and growth of fat crystals began to limit the flow of PEGs, so the modulus of PEGs increased. The scaffold network of PKST can be observed by microscopy (Figure S3b). When the proportion of PKST in soybean oil was 0%, only pure PPs attached to the interface of emulsion droplets and the stacked emulsion droplets could be imaged by the polarized light microscope. When the PKST proportion increased to 25%, the continuous phase was filled with fat crystals and crystals further grew and formed larger clusters as the PKST proportion became 50%. The number of crystal clusters kept increasing and growing following the addition of more PKST. During the rheological cooling test, the modulus of PEGs containing 25% PKST in the oil phase was only higher than that containing neat soybean oil in the cooling process, but their G' was

almost the same at 20 ºC indicating that the network structure formed by tiny fat crystals had limited resistance to shear. More crystals and larger crystal clusters were generated when the proportion of PKST was higher than 50%, resulting in a significant impact on the rheological properties of PEGs. After cooling from 50 ºC to 20 ºC, G' of PEGs with neat PKST jumped from less than 10,000 Pa to more than 100,000 Pa, in line with the transformation of PEGs from soft solids to hard solids. Since the system was utterly solidified at temperatures lower than 20 ºC, and PEGs showed very little fluidity, the lower limit of the test was 20 ºC. The hardness of PEGs was measured by the texture analyzer after their complete solidification (Figure 3c). The vertical force causing 30% deformation of PEGs was only less than 100 g in the PEG prepared using neat soybean oil. The hardness of PEGs increased exponentially with the increase of PKST concentration in the oil phase, which showed that the scaffold structure formed by fat crystals reinforced the PEGs. For neat PKST, the vertical force causing 30% deformation exceeded 12,000 g, providing great potential for non-toxic PEGs to play a role in tissue engineering.[34, 35]

is it possible that crystals of PKST **also** adsorb on water droplets after cooling?

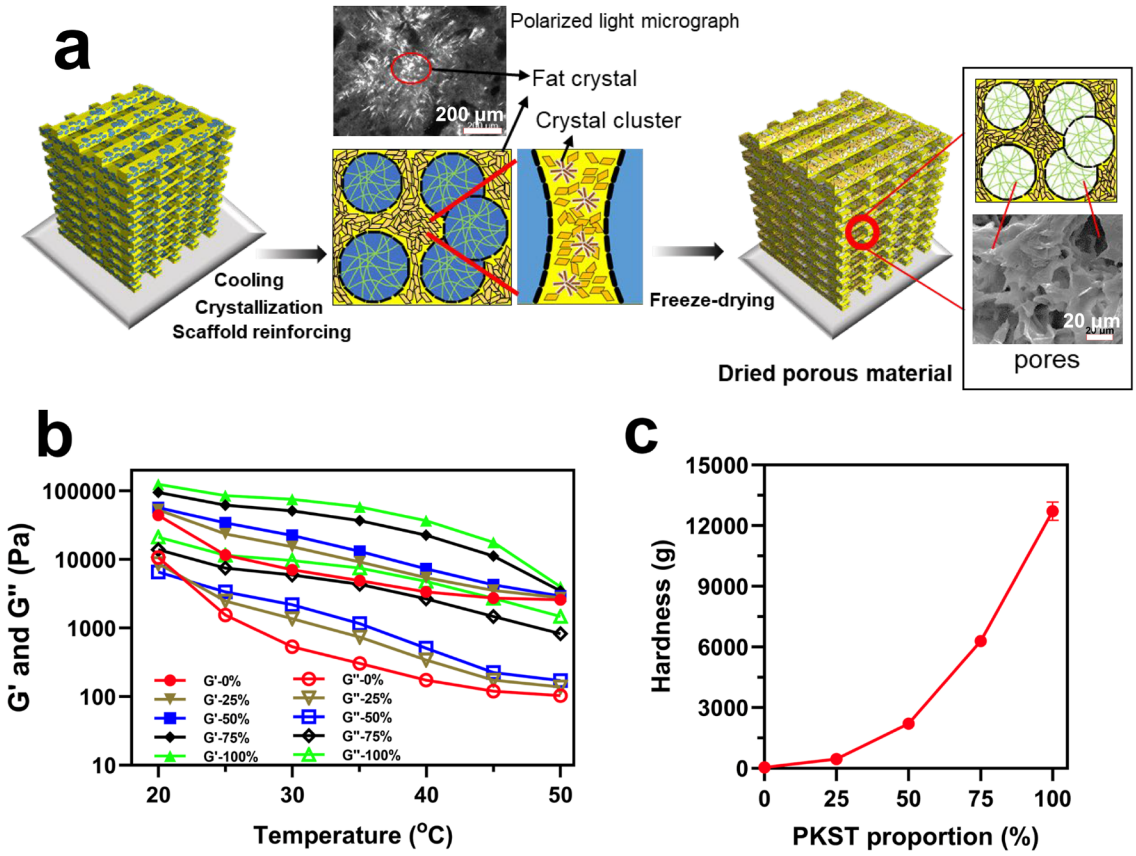

Figure 3. (a) Illustration of the scaffold reinforcing in PEGs by PKST crystals and crystal clusters and the preparation of fat crystal network-based porous materials by freeze drying, (b) variation of G'' and G' with temperature for PEGs having different proportions of PKST in the oil phase, (c) hardness of solidified PEGs as a function of the proportion of PKST in oil.

2.4. Model customizing and 3D printing of PEGs

As people pay more and more attention to private customized products, the market for the personalized service shows a great expansion and a variety of forms for customizing appear. As a convenient, fast and creative food manufacturing method, food 3D printing is becoming more and more popular.[36] Generally, equipment manufacturers of food 3D printers can only provide existing models for 3D printing. Factors such as the technical threshold of modeling greatly limit people's imagination and restrict the creativity of food 3D printing. The optical 3D scanning imager is a real-time and fast tool to achieve customization, which can model the object by optical scanning technology. Therefore, this work used a handheld 3D scanning imager for the rapid modeling (Figure 4a), and a simple version of the Eiffel Tower was taken as the target to create the digital model (Figure 4b). PEGs containing different proportions of PKST were 3D printed based on the digital model (Figure 4c). PEGs could carry out DIW printing of this model (Video S1), but to maintain the partially hollowed out structure , PKST needed to give full play to the advantages of the fused deposition modeling (FDM) re-write as very unclear. PEGs prepared with neat soybean oil could not hold the structure in printing the hollow shape, and the printed object collapsed during printing. After adding 25% PKST to the oil, the printed object could be printed entirely but still collapsed after tilting the model by 45°. As the PKST proportion became 50%, the printed object retained structural integrity after being tilted by 45° although a slight deformation occurred. High proportions of PKST (75% and 100%) endowed the printed object with solid characteristics such that they did not suffer after 90° inclination. The object printed by the PEG with 75% PKST had a smoother appearance than that printed by the PEG with 100% PKST, which was due to the smaller G' and better fluidity of the former. Obviously, the reinforcing effect of the scaffold network formed by fat crystals from PKST in PEGs by combining the superiority of DIW and FDM could greatly meet the needs of expanding the creativity for edible 3D printing re-write to clarify. Moreover, using high internal phase emulsions means a low oil content, meeting the concept of a healthy diet

pursued by consumers.

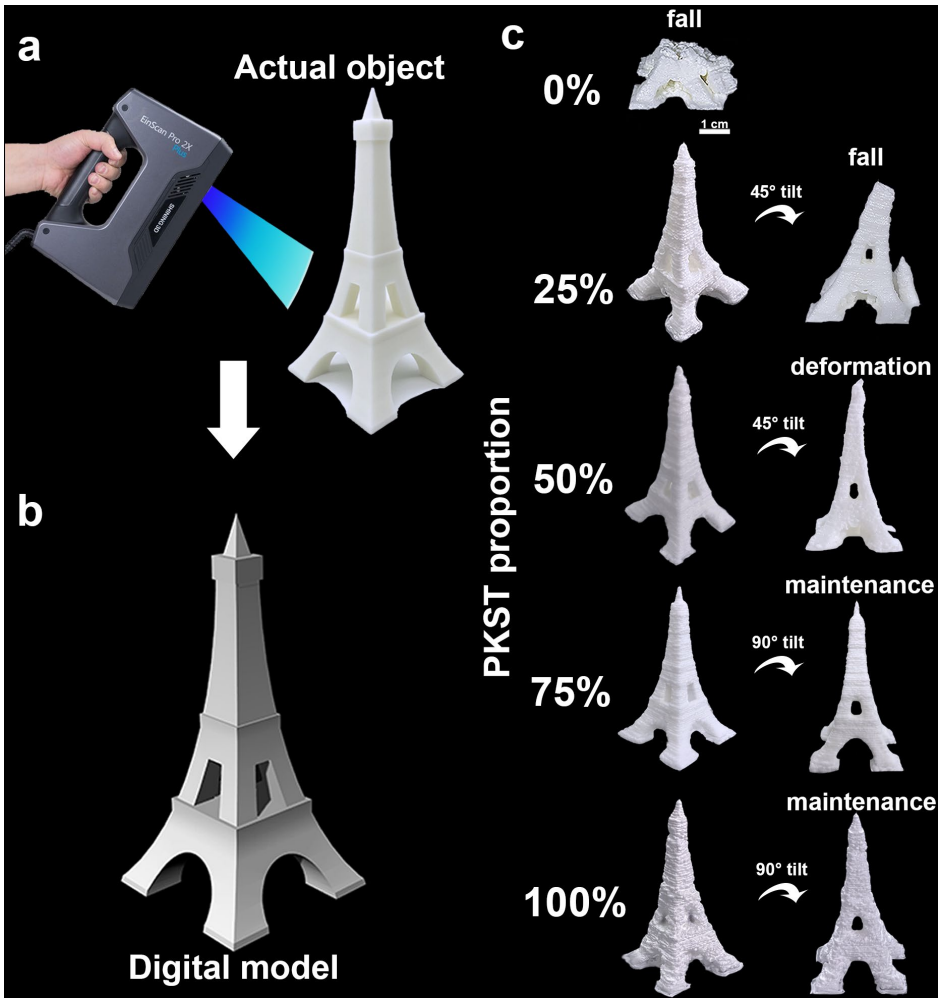

Figure 4. (a) Scanning of the simple Eiffel Tower with the handheld scanning imager, (b) digital model obtained from the handheld scanning imager, (c) printed objects using PEGs containing different proportions of PKST in oil and after tilting by 45º and 90º.

2.5. Rigid edible-grade porous materials from PEG template

Porous materials, such as aerogels, are widely used in all aspects of daily life such as thermal insulation, separation, sorption, catalysis, medicine and food.[37] Porous materials prepared using an emulsion template are commonly encountered if a monomer oil phase is used which polymerises subsequently giving rise to the walls of the pores.[37, 38] In this work, the continuous phase of PEGs was used as the rigid scaffold and water within the droplets was removed to generate pores. The scaffold network self-assembled by fat crystals from PKST in PEGs contributed significantly to the structural strength of porous materials prepared by the PEG-

templated method. A ring-shaped Hibert curve was adopted as the digital model for 3D printing using PEGs (Figure 5a(i and ii)), and a weight of 500 g was used to test the strength of printed objects (Figure 5a(iii)). The printed object from PEGs containing less than 50% PKST in oil could not support the weight, and that with 75% PKST could hold the weight to a certain extent but it would fail to hold it in the end. The printed object from the PEG with 100% PKST could completely bear the weight of 500 g. Porous materials were fabricated by freeze drying PEGs *in-situ* what does this mean? to obtain the pore structure after removing water. As soybean oil has no fat crystal scaffold to support the object, the printed structure of the PEG prepared using neat soybean oil seriously collapsed after freeze drying, and the outline of emulsion droplets disappeared completely under cryo-SEM investigation (Figure 5b(i)). When the PKST proportion in the oil phase increased to 25%, the appearance of the freeze dried PEG showed it was partially deformed and the outline of emulsion droplets was retained in part (Figure 5b(ii and iii)). However, the pore size profile was larger than that of the original emulsion droplets, meaning that coalescence of emulsion droplets occurred during freezing and drying. When the PKST proportion was higher than 50%, the shape of the printed objected could be saved and the outline of emulsion droplets was clearly visible in the cryo-SEM. The higher the PKST proportion in the oil phase, the more intact pores retention was what is this?, the closer the pore size was to the size of emulsion droplets in the precursor PEGs. Adjusting the properties of templates to affect the properties of subsequent products is an effective means to fabricate designated products by the templated approach.[39, 40] Hence, in the preparation of rigid porous materials from a PEG template, due to the influence of the PKST proportion in oil on the integrity of pores derived from emulsion droplets, the pore size of the food grade porous material could be controlled.

have you measured the pore size distribution for the different porous materials?

you need some more SEM images of the porous materials to be convincing

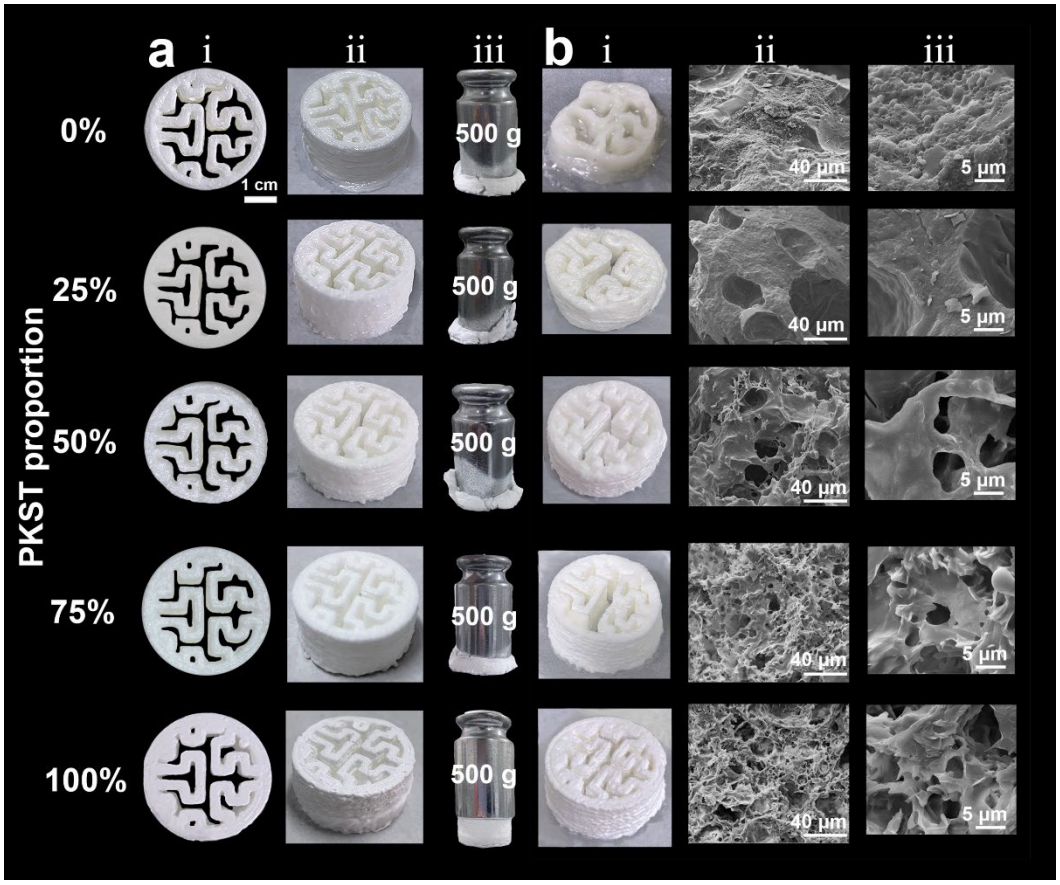

Figure 5. (a) i and ii Printed ring-shaped Hibert curve using PEGs containing different proportions of PKST in oil, iii extrusion test using a 500 g weight. PEG with neat PKST can support the weight, (b) i freeze dried printed objects and ii, iii associated cryo-SEM images.

2.6. Design of thermally actuated 4D printing

4D printing has an additional dimension compared with traditional 3D printing which is time, meaning that the 3D printed object can change spontaneously with time under certain environmental conditions. Primary factors in advanced food 4D printing that could trigger the variety of objects are the moisture content and the environmental temperature.[41] Vegetable paste with a high moisture content could be dehydrated by different methods to achieve the deformation. For example, the 3D printed object of potato paste could be microwave heated removing water and realizing the effect of 4D printing.[14] Due to the chemical reaction between polysaccharides and proteins at high temperature, dough showed the potential for 4D printing by baking.[42, 43] These deformation forms largely depend on the directional shrinkage of the material during dehydration, while chocolate products with high solid fat content depend on the melting destruction of the fat crystal network by heating.[44] Hence, products containing fats

with a high melting point would need to design the actuating force in the digital model reasonably and use gravity for the deformation in 4D printing. 4D printing of PEGs was also realized based on the destructive effect of heating the scaffold network of fat crystals formed by PKST, meaning that thermally actuated 4D printing should combine characteristics of digital models and gravity. In this work, the PEG with neat PKST as the oil phase was used to carry out 4D printing for the process of flower blooming (Figure 6 and Video S2). Each petal of the 3D printed flower was independent of each other and then placed on the heating plate at 50 °C for deformation need to describe each part of Figure 6 sequentially (Figure 6e and Video S3). Meanwhile, the infrared thermal imager was used to monitor the temperature of the 3D printed flower during deformation (Figure 6d). With the gradual heating and softening of the root of the petal, G' of the bottom decreased. At the action of the component of gravity re-phrase, which was the parallel stress on the petal, the shear strain occurred at the bottom. The design of the petal tilt was essential because it determined the gravity component deciding the parallel stress on the bottom of the petal (Figure 6a). The model was designed using:[45]

$$\frac{\sigma}{\varepsilon} = G \tag{2}$$

where σ, ε and G represent the stress, strain and shear modulus, respectively. Also,

$$\sigma = \frac{\tau}{A},\ \ \varepsilon = \tan\gamma,\ \ G = \frac{E}{2(1+v)} \tag{3}$$

where τ is the parallel force, A is the stressed area, γ is the angle of the strain, E is the elastic modulus and v is the Poisson ratio. As for PEGs, the Poisson ratio was considered to be 1 due to the liquid nature of water and oil. If the angle between the petal and the plane at the beginning was a and the mass of the petal was M, then the vertical force on the center of gravity of the petal was $Mg(sin(a))$ (radial force). According to the length conversion of the force arm, it was assumed that the radial force (τ) on the force point at the bottom of the petal was

$$\tau = kMg\sin(\alpha) \tag{4}$$

where k is the conversion factor of the force arm. Then, the relation between the elastic modulus of the PEG and the strain at the bottom of the petal can be obtained:

$$\varepsilon = \frac{kMg\sin(\alpha)}{AE} \tag{5}$$

Polynomial fitting was performed on the results of the temperature rheological sweep for the PEG to obtain the elastic modulus ($y_{(T)}$) as a function of temperature (T) from 20 to 50 °C (Figure 6b). Hence, the relation between the strain angle and the temperature of the bottom of the petal was

$$\gamma = \arctan\left(\frac{kMg\sin(\alpha)}{Ay_{(T)}}\right) \tag{6}$$

what do you do with these eqns. which are derived here? It could be assumed that petals would fall irreversibly at a certain strain angle generated at the bottom. Hence, in modeling for 4D printing of PEGs, the control of the object deformation at a certain temperature could be determined by the shape, mass, initial inclination angle and the area subjected to the radical force, respectively.

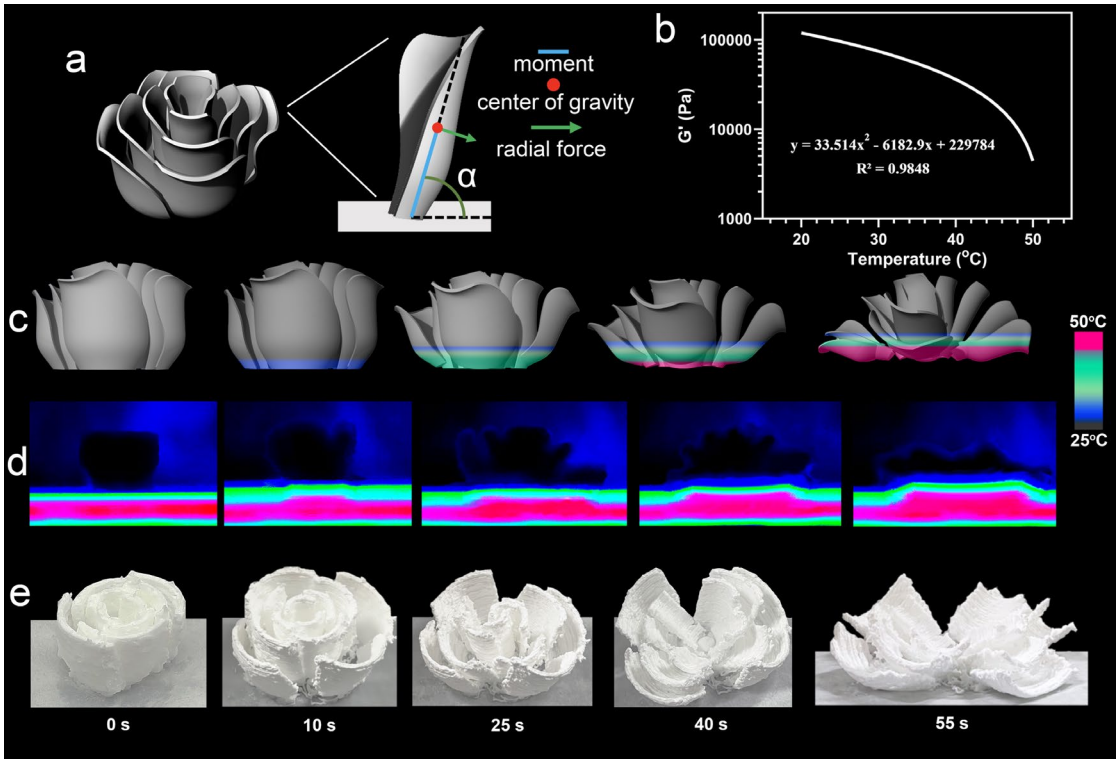

Figure 6. (a) Digital model and stress analysis of 4D printing using PEGs, (b) polynomial fitting of the temperature rheological sweep data of the PEG with neat PKST as the oil phase, (c) schematic of the heat absorption and variation of the digital model in the heating process, (d)

monitoring of the heat absorption of the printed object by an infrared thermal imager, (e) appearance of the printed flower recorded at different times after placing on a 50 ºC heating plate. The printed flower is actuated due to the thermal sensitivity of PKST.

2.7. Application of PEGs in 4D printing of chocolate

The PEG with neat PKST as the oil phase is a high internal phase water-in-oil emulsion gel, and could be mixed evenly with cocoa butter before PKST reinforces the PEG by cooling letting the PEG can partially replace the cocoa butter unclear- re-phrase what you want to say in the preparation of chocolate products so as to reduce the total content of fat. The molded chocolate fabricated by the mixed cocoa butter that had 30 wt.% PEG containing neat PKST had an ordinary appearance very unclear what mixtures you have made: this needs to be clearer (Figure 7a). However, there were many water droplets inside the chocolate, making the chocolate be low calorie products??. It could be found from the cryo-SEM of the freeze dried chocolate that there were many pores inside, which were initially the location of water droplets. 3D printing of chocolate products is also a popular topic.[46] Therefore, the impact of the PEG-replaced cocoa butter on the 3D printed chocolate was tested (Figure 7b). The logo of Jiangnan University and the outer wall were printed by the 3D printer, and then they were assembled together to achieve a simple 4D printing effect. When the bottom of the target was heated, the outer wall gradually melted and dropped and the internal logo appeared (Video S4). The replacement of cocoa butter by PEG in preparing chocolate products maintained the basic properties of chocolate in both molding and 3D printing and also reduced the total fat content in the chocolate. Hence, a PEG is a potential low fat substitute to replace high saturated and trans fats catering to the low calorie and healthy diet concept.

Figure 7. (a) Appearance and cryo-SEM image of molded chocolates with 60 wt.% mixed cocoa butter that has 30% PEG (neat PKST as oil phase), (b) 4D printing effect of the PEG-containing chocolate to reveal the Jiangnan University logo on the 50 ºC heating plate; the used chocolate had 75 wt.% mixed cocoa butter that has 30% PEG (neat PKST as oil phase).

3. Conclusions I will edit this in next draft

Phytosterol nanoparticles (PPs) stabilized high internal phase (75%) water-in-oil Pickering emulsion was gelled due to the first scaffold network generated by jammed emulsion droplets and hydrogen bonding among PPs, making it have unique thixotropy (fluidity) and structural recovery ability (plasticity) that was ideal properties for the ink of DIW 3D printing. The Pickering emulsion gel (PEG) could be further reinforced by the second scaffold network of fat crystals formed by palm kernel stearin (PKST) in the continuous oil phase, transforming the edible-grade PEG from the viscoelastic semi-solid nature to the rigid solid. The reinforcement effect of the crystal scaffold network in PEGs was combined with the real-time modeling technology to achieve more challenging food 3D printing. The crystal scaffold network in the continuous oil phase could greatly increase the strength of printed objects, which was better than most of the soft solid for edible 3D printing in shaping. The 3D printed PEG template was used to prepare rigid porous materials based on the reinforced scaffold network of crystals in PEGs, and the microstructure of the porous material could be regulated by changing the PKST proportion in the oil phase for meeting the requirement of customizing specific functional materials. By controlling the stress design of the printing target and combined with the thermal-induced modulus change of PEGs, the thermally actuated 4D printing was conducted. The low oil content of PEGs enabled PEGs to fabricate fat-reducing health foods by advanced production technology (3D/4D printing). The PEG, containing PKST as the outer oil phase, can be widely adopted in bioengineering, food, medicine, personal care, and many fields because of its excellent biocompatibility and edibility. The highly customized function provides a good platform for the development of applications using the PEG template.

4. Experimental

Materials: The phytosterol was purchased from Healthful Biotech (Xian, China). Palm

kernel stearin (PKST, melting point = 33 ºC (Figure S4)), refined soybean oil, cocoa butter and cocoa powder were obtained from Yihai Kerry (Shanghai, China) as gifts. κ-carrageenan was purchased from Greenfresh (Fujian, China). Other reagents used were obtained from Macklin (Shanghai, China).

Methods: *Preparation of phytosterol particle suspension*: Phytosterol nanoparticles (PPs) were fabricated using the anti-solvent precipitation method.[47] 2 wt.% of native phytosterol was dissolved in pure ethanol at 45 ºC. The ethanol solution was mixed 1:1 (w/w) with 0.1 M PBS (pH 7) and immediately homogenized using a homogenizer (T25, IKA, Germany) at 16,000 rpm for 4 min. A rotary evaporator (RV8, IKA, Germany) was used to remove ethanol and concentrate PPs to 4 wt.%.

Microscopy of PPs: Microscopy of freeze-dried need clear details on freeze drying (20F/A, SCIENTZ, China) PPs was performed using a scanning electron microscope (SEM, SU8100, Hitachi, Japan) at 3-5 kV accelerating voltage. Flaky particles were analyzed by Image J (NIH, USA) to obtain the size and thickness data.

Three-phase contact angle of particles: A hydraulic tablet press was used to make the phytosterol sheet from what?, which was then immersed in soybean oil. A ? μL water drop was then formed under oil. The sessile drop method was used to measure the three-phase contact angle using the optical-contact angle measuring tester (OCA15EC, Dataphy, Germany).

Preparation of water-in-oil Pickering emulsion gel: 0.3 wt.% κ-carrageenan was added into an aqueous PP suspension, which was mixed with oil at 75%:25% (v/v) in a 45 ºC water bath. The mixture was homogenized at 11,000 rpm for 4 min to obtain the Pickering emulsion gel (PEG). The oil phase was either neat soybean oil or mixtures with PKST where the content of PKST varied from 25, 50, 75 and 100% (vol.).

Droplet size distribution: Microscopy of emulsion droplets was observed using a cryo-scanning electron microscope (Cryo-SEM, Quorum PP3000T, Shiyanjia Lab, China), a confocal laser scanning microscope (CLSM, LSM-880, Zeiss, Germany) and a polarized light microscope (DM2500P, Leica, Germany). The PEG was freeze-dried details? before being captured for cryo-SEM (5-10 kV accelerating voltage). The oil phase and PPs were stained by Nile Red and Rhodamine B, respectively. The droplet size distribution was determined using Image J.

FTIR analysis: Freeze-dried PPs, κ-carrageenan powder and freeze-dried PEGs were swept by the attenuation reflection accessory of the infrared spectrometer (IS-10, Nicolet, USA) from 4000 to 550 cm^{-1}.

Rheological and textural measurement: A rotational rheometer (DHR-3, TA, USA) was used to scan PEGs. The strain sweep began from 0.01 to 100%, and the frequency and temperature were 1 Hz and 45 ºC, respectively. The time sweep was the three-stage jump sweep and had twice strain shock at 60 and 110 s, respectively. The first shock turned the strain from 0.01 to 100% while the second turned the strain from 100 back to 0.01% (frequency 1 Hz, temperature 45 ºC). The temperature sweep was from 50 to 20 ºC, with the strain and frequency at 0.01% and 1 Hz, respectively. The testing gap of the rheometer was 1000 μm, and the utilized planar probe had a 40 mm diameter. The hardness of solidified PEGs was measured by the SMS texture analyzer describe briefly what is done (TAXT, British) at 25 ºC, and the vertical force that would result in 30% strain is reported as the hardness of PEGs.

Model customizing and 3D printing: The digital model file was obtained by scanning a real object using the handheld 3D scanning imager (EinScan-Pro 2X-plus, Shining, China). 3D printing of PEGs was performed by a 3D food printer (Shinnove-E1, Hangzhou Panda, China). The temperature of the ink storage tank was 45 ºC. The diameter of the nozzle was 0.85 mm.

Preparation of porous materials: PEGs comprised of various oil phases were 3D printed to create objects, which then were frozen at -80 ºC for 20 min and freeze-dried for 48 h to obtain water-free porous materials.

4D printing of PEGs and application in chocolate: Models for 4D printing were designed by Rhinoceros 5.0 (Robert McNeel, USA). Models were printed by the 3D food printer and placed on the table for 1 h at 25 ºC to solidify printed objects. Then these printed objects were put on a hotplate at 50 ºC for the deformation, and the whole process was recorded by a thermal infrared camera (A3D-13, iRay, China). In the use of the pouring method to prepare chocolate, (60 wt.% mixed cocoa butter, 15 wt.% cocoa powder and 25 wt.% sugar), mixed cocoa butter had 30 wt.% PEG (containing neat PKST as oil). The cocoa butter was heated and melted in a 60 ºC water bath, and was then mixed evenly with the freshly prepared PEG. Cocoa powder and sugar were added into the mixed cocoa butter alongwith uniform stirring. The mixture was then poured into the mold and placed in a 25 ºC thermostat for 1 h to prepare the chocolate. In

3D printing (40 °C) to prepare chocolate, (75 wt.% mixed cocoa butter, 10 wt.% cocoa powder and 15 wt.% sugar), mixed cocoa butter had 30 wt.% PEG (containing neat PKST as oil). The cocoa butter was heated and melted in a 60 °C water bath, and was then mixed evenly with the freshly prepared PEG. Cocoa powder and sugar were added into the mixed cocoa butter alongwith uniform stirring. The mixture was added to the 3D food printer for printing chocolate. The diameter of the nozzle was 0.85 mm.

Acknowledgments

This research was supported by the National Natural Science Foundation of China (31972112), the National Natural Science Foundation of China (31772008) and by Jiangsu Province Science and Technology Plan Project (BE2019369).

References you need titles of all the papers

[1] B. Wu, C. Yang, Q. Xin, L. Kong, M. Eggersdorfer, J. Ruan, P. Zhao, J. Shan, K. Liu, D. Chen, D. A. Weitz, X. Gao, *Adv. Mater.* **2021**, 33, 2102362.
[2] A. R. Patel, *Adv. Funct. Mater.* **2018**, 30, 1806809.
[3] Y. Chevalier, M.-A. Bolzinger, *Colloids Surf. A* **2013**, 439, 23.
[4] J. Tang, P. J. Quinlan, K. C. Tam, *Soft Matter* **2015**, 11, 3512.
[5] H. Wu, X. Du, X. Meng, D. Qiu, Y. Qiao, *Nat. Commun.* **2021**, 12, 6113.
[6] W. W. Mwangi, H. P. Lim, L. E. Low, B. T. Tey, E. S. Chan, *Trends Food Sci. Technol.* **2020**, 100, 320.
[7] F. Ravera, K. Dziza, E. Santini, L. Cristofolini, L. Liggieri, *Adv. Colloid Interface Sci.* **2021**, 288, 102344.
[8] T. D. Ngo, A. Kashani, G. Imbalzano, K. T. Q. Nguyen, D. Hui, *Composites, Part B* **2018**, 143, 172.
[9] L. Y. Zhou, J. Fu, Y. He, *Adv. Funct. Mater.* **2020**, 30, 2000187.
[10] X. Wang, M. Jiang, Z. Zhou, J. Gou, D. Hui, *Composites, Part B* **2017**, 110, 442.
[11] T. Billiet, E. Gevaert, T. De Schryver, M. Cornelissen, P. Dubruel, *Biomaterials* **2014**, 35, 49.
[12] C. He, M. Zhang, Z. X. Fang, *Crit. Rev. Food Sci. Nutr.* **2020**, 60, 2379.
[13] C. Minas, D. Carnelli, E. Tervoort, A. R. Studart, *Adv. Mater.* **2016**, 28, 9993.
[14] C. He, M. Zhang, S. Devahastin, *ACS Appl. Mater. Interfaces* **2020**, 12, 37896.
[15] J. Du, H. J. Dai, H. X. Wang, Y. Yu, H. K. Zhu, Y. Fu, L. Ma, L. Peng, L. Li, Q. Wang, Y. H. Zhang, *Food Hydrocolloids* **2021**, 113, 106536.
[16] B. Jiao, A. Shi, Q. Wang, B. P. Binks, *Angew. Chem. Int. Ed.* **2018**, 57, 9274.
[17] A. G. Marangoni, J. P. M. van Duynhoven, N. C. Acevedo, R. A. Nicholson, A. R. Patel, *Soft Matter* **2020**, 16, 289.
[18] S. Sridharan, M. B. J. Meinders, L. M. Sagis, J. H. Bitter, C. V. Nikiforidis, *Adv. Funct.*

Mater. **2021**, 31, 2101749.
[19] E. Dickinson, *Curr. Opin. Colloid Interface Sci.* **2010**, 15, 40.
[20] L. Bai, S. Huan, W. Xiang, O. J. Rojas, *Green Chem.* **2018**, 20, 1571.
[21] U. Makhmudova, P. C. Schulze, D. Lutjohann, O. Weingartner, *Curr. Atheroscler. Rep.* **2021**, 23, 68.
[22] F. Liu, C. H. Tang, *J. Agric. Food Chem.* **2014**, 62, 5133.
[23] Y. Wang, C. Yuan, B. Cui, Y. Liu, *Carbohydr. Polym.* **2018**, 202, 530.
[24] Q. Jiang, S. Li, L. Du, Y. Liu, Z. Meng, *J. Colloid Interface Sci.* **2021**, 602, 822.
[25] J. Texter, *Curr. Opin. Colloid Interface Sci.* **2015**, 20, 454.
[26] G. Cavallaro, S. Milioto, L. Nigamatzyanova, F. Alchatova, R. Fakhrullin, G. Lazzara, *ACS Appl. Nano Mater.* **2019**, 2, 3169.
[27] Z. Liu, M. Zhang, B. Bhandari, Y. Wang, *Trends Food Sci. Technol.* **2017**, 69, 83.
[28] H. Yuk, X. Zhao, *Adv. Mater.* **2018**, 30, 1704028.
[29] Y. Cao, R. Mezzenga, *Nat. Food* **2020**, 1, 106.
[30] M. Davidovich-Pinhas, S. Barbut, A. G. Marangoni, *Annu. Rev. Food Sci. Technol.* **2016**, 7, 65.
[31] L. Du, S. Li, Q. Jiang, Y. Tan, Y. Liu, Z. Meng, *Food Hydrocolloids* **2021**, 117, 106737.
[32] G. F. L. Koay, T.-G. Chuah, T. S. Y. Choong, *Ind. Crops Prod.* **2013**, 49, 437.
[33] F. Zhang, J. Li, S. Yang, Y. Bi, *Fuel* **2021**, 297, 120782.
[34] L. F. Hartje, C. D. Snow, *Wiley Interdiscip. Rev.: Nanomed. Nanobiotechnol.* **2019**, 11, e1547.
[35] J. Yang, J. Wang, B. Hou, X. Huang, T. Wang, Y. Bao, H. Hao, *Chem. Eng. J.* **2020**, 399, 125873.
[36] C. Y. Feng, M. Zhang, B. Bhandari, *Crit. Rev. Food Sci. Nutr.* **2019**, 59, 3074.
[37] S. Y. Zhao, W. J. Malfait, N. Guerrero-Alburquerque, M. M. Koebel, G. Nystrom, *Angew. Chem. Int. Ed.* **2018**, 57, 7580.
[38] Z. Tian, Y. Zhao, S. Wang, G. Zhou, N. Zhao, C.-P. Wong, *J. Mater. Chem. A* **2020**, 8, 1724.
[39] Q. Jiang, P. Li, M. Ji, L. Du, S. Li, Y. Liu, Z. Meng, *Food Chem.* **2021**, 372, 131357.
[40] Q. Jiang, L. Du, S. Li, Y. Liu, Z. Meng, *Food Hydrocolloids* **2021**, 120, 106901.
[41] C. Chen, M. Zhang, C. Guo, H. Chen, *Innovative Food Sci. Emerging Technol.* **2021**, 68, 102605.
[42] L. L. Zhao, M. Zhang, B. Chitrakar, B. Adhikari, *Crit. Rev. Food Sci. Nutr.*, https://doi.org/10.1080/10408398.2020.1799327.
[43] Y. Tao, Y. C. Lee, H. Liu, X. Zhang, J. Cui, C. Mondoa, M. Babaei, J. Santillan, G. Wang, D. Luo, D. Liu, H. Yang, Y. Do, L. Sun, W. Wang, T. Zhang, L. Yao, *Sci. Adv.* **2021**, 7, eabf4098.
[44] M. L. 3D-Studio, The First Chocolate 3D-Printing Studio in the World, https://www.barry-callebaut.com/en/artisans/mona-lisa/3dstudio, accessed: 11, Access **2021**.
[45] R. G. Larson, *The Structure and Rheology of Complex Fluids*, Oxford University Press, New York, **2000**.
[46] S. M. Kim, J. H. Woo, H. W. Kim, H. J. Park, *J. Food Eng.* **2022**, 314, 110785.
[47] M. Lan, Y. Song, S. Ou, J. Zheng, C. Huang, Y. Wang, H. Zhou, W. Hu, F. Liu, *Langmuir* **2020**, 36, 14991.

TOC

Double Scaffold Networks Regulate Edible Pickering Emulsion Gel for Designing Thermally Actuated 4D Printing

Qinbo Jiang, Bernard P. Binks and Zong Meng*

An edible water-in-oil Pickering emulsion gel reinforced by a crystal scaffold has been designed. The crystal network in the oil phase can alter the system strength by control of the temperature, realizing more challenging food 3D/4D printing. Moreover, customizable and rigid porous materials have been fabricated from the emulsion template.

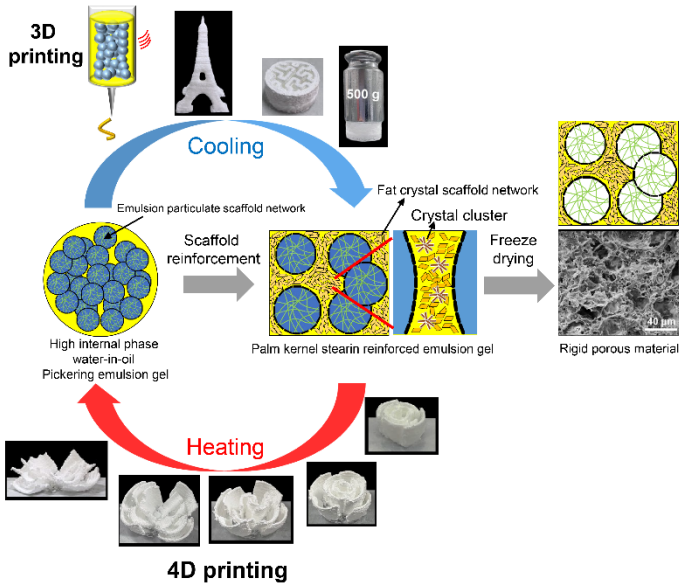

I think this is too big for most journal TOC images
it needs to be smaller and simpler